Nuclear charge distribution of fission products from ^{235}U(n_{th}, f) of the masses 79 to 100

G. Siegert,* H. Wollnik, J. Greif,† R. Decker, G. Fiedler, and B. Pfeiffer

II. Physikalisches Institut der Universität, 6300 Giessen, Germany

(Received 14 January 1976)

Passing mass separated recoil fission particles through a ΔE Si-surface barrier detector the nuclear charge distributions of fission products were measured in the mass chains 79 to 100. The average nuclear charge as well as the second, third, and fourth moment of the nuclear charge distribution reveal odd-even and shell effects.

NUCLEAR REACTION, FISSION ^{235}U(n_{th}, f), measured nuclear charge distribution of $A = 79$ to $A = 100$, deduced element and isotone yields, proton and neutron odd-even effect.

I. INTRODUCTION

The knowledge of nuclear charge distributions of fission products from ^{235}U(n_{th}, f) has been based for many years on radiochemical methods.[1] In most cases only a few of the independent yields could be determined for each isobaric chain. The general features, however, were still seen, and it was concluded that fission products with even proton numbers are produced more abundantly than fission products with odd ones.[1]

A quite different approach to determine nuclear charge distributions was to use recoil separators. With such a separator the nuclear charge distributions of fission products were determined for a few masses A as a function of the excitation of the fragments.[2] From these results it was seen that in even A nuclei, the formation of even-even nuclei is favored at low excitation energy since the small amount of energy available reduces the probability of breaking nucleon pairs which is necessary to form odd-odd nuclei. With the low intensity available at that mass separator only nuclear charge sensitive detectors with large areas could be used such as nuclear emulsions or gas and scintillation counters[3] to record the total number of β rays emitted from one fission product and from its daughters. Attempts to observe the nuclear charge dependent energy deposit in an 8 μm thick ΔE Si-surface barrier detector gave no results due to the small area available and due to the low particle intensity. Experiments with a gas filled magnetic recoil separator had much higher intensities. However, at this separator a separation of neighboring masses was not possible because of the limited mass resolving power. Therefore only results averaged over several masses could be obtained.[4]

When the new recoil mass separator LOHENGRIN in Grenoble came into operation[5] the 8 μm thick

ΔE Si-detector mentioned above was employed successfully[6] to separate neighboring nuclear charges. More recently another method had also been used to observe the nuclear charge dependent energy loss in thin foils by determining the velocity of the slowed down fission products.[7] Both methods were applied successfully to determine the nuclear charge distributions of fission products of the light group provided by LOHENGRIN. From such measurements new features of the nuclear charge distributions were derived.[7-14]

II. EXPERIMENTAL PROCEDURE TO DETERMINE NUCLEAR CHARGE DISTRIBUTIONS

The recoil separator LOHENGRIN installed at the high flux reactor in Grenoble separates fission products according to their masses, kinetic energies, and ionic charges.[5] It is a modified version[15] of the classical Kauffmann-Thomson parabola spectrograph. For properly chosen parameters it has a mass resolving power of $A/\Delta A = 800$ and an energy resolving power of $E/\Delta E = 300$, both resolutions being taken for full width at 1/10 of the maximum [FW(1/10)M]. This mass resolving power is high enough to separate neighboring mass to charge ratios of fission products.

To determine the nuclear charge distribution of fission products of one mass and fixed energy, the particles were shot through a ΔE Si-surface barrier detector recording the individual energy loss. For measurements which identify nuclear charges of fission products by energy loss the high energy resolving power of 300 used here turned out to be essential. To minimize the effect of a thickness variation of the detector, its thickness was chosen[6] to be 8 μm which corresponds to about half of the penetration depth of fission products. As an example, the resulting pulse height distribution is shown in Fig. 1 for particles of mass $A = 97$.
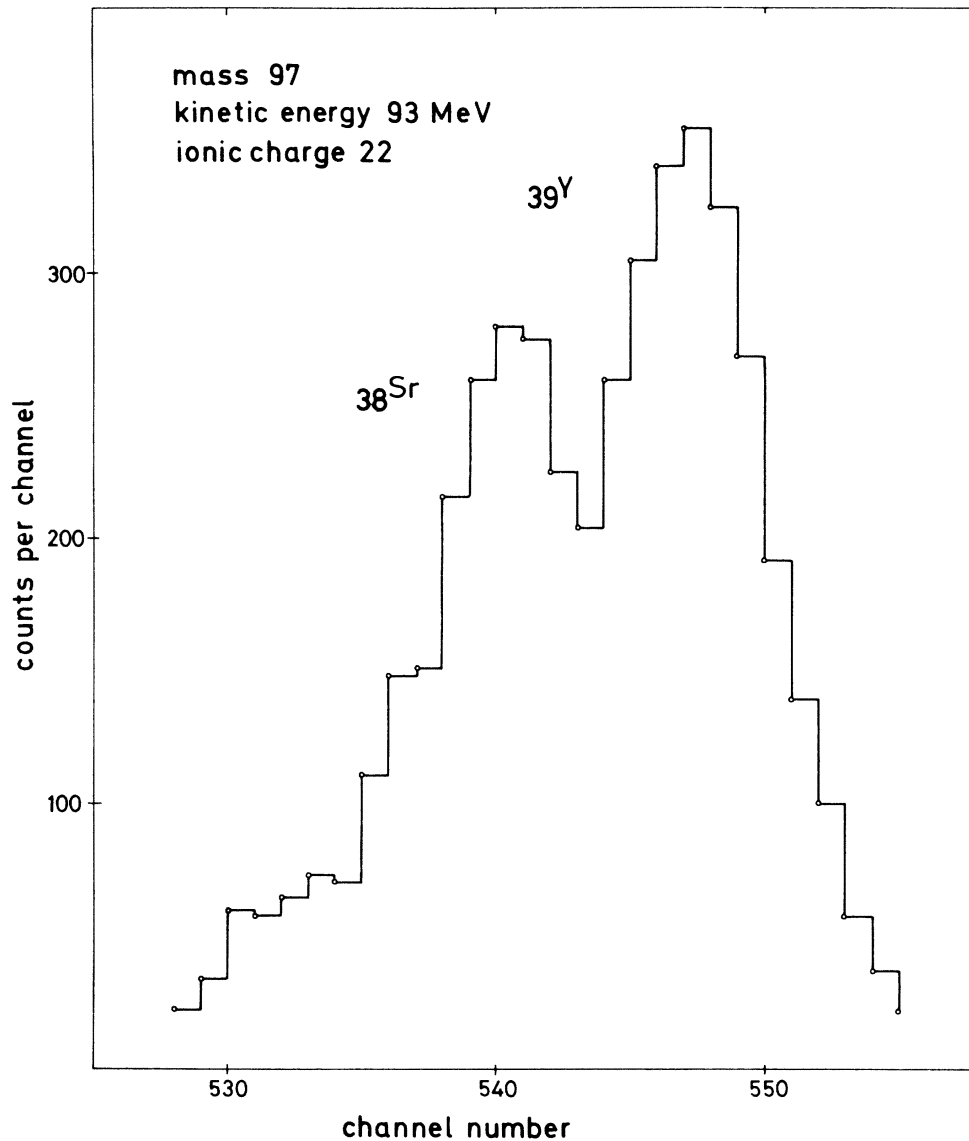
FIG. 1. The signal obtained from a ΔE Si-surface barrier detector irradiated by monoenergetic fission products of mass 97. One can clearly distinguish the peaks due to ^{97}Y and ^{97}Sr. The peak due to ^{97}Rb is still noticeable as a shoulder.

The pulse height distribution for one nuclear charge was found to be Gaussian with no detectable tailing within the statistical limits. The obtained nuclear charge resolving power was 43 [full width at half maximum (FWHM)] or 24 [FW(1/10)M] for particles of 90 MeV energy. If very low yields have to be recorded in the wings of much more abundant ones the unfolding procedure becomes difficult and increasingly less reproducible. As it was shown in Ref. 6 the reproducibility for yields of several percent was rather good. Below that limit the reproducibility is less satisfying and demands an increase of the statistical error given in Table I by perhaps 0.3%. However, none of the following results depend on these very low yields.

III. RESULTS AND DISCUSSION

The measured nuclear charge distribution for each isobar was obtained by unfolding the measured pulse height distribution by a set of equally spaced Gaussians of constant half width fitted to the data. This fitting procedure was applied to the data of each isobar for varying kinetic energies and varying ionic charges.

TABLE I. The relative yields of the different elements within the isobars $A = 79$ to $A = 100$. In a separate column the average nuclear charge Z_a is listed for each isobaric chain. The values in brackets are taken from Ref. 17.

A \ Z	30	31	32	33	34	35	36	37	38	39	40	41	42	Z_a
79	3.7±1.5	37.8±4.0	52.5±5.0	6.0±2.0										31.51
80		9.7±2.5	83.2±4.0	7.1±2.0										31.97
81		4.9±1.5	64.4±3.0	26.6±2.5	4.1±1.5									32.30
82		2.1±1.0	39.5±3.0	47.2±3.0	9.5±1.5	1.7±1.0								32.69
83			9.7±1.0	56.0±2.0	31.2±2.0	3.1±1.0								33.28
84			2.3±0.7 (3±)	23.5±1.4 (37±6)	69.2±2.5 (57±6)	5.0±1.0 (3±2)								33.77
85			1.2±0.5	11.4±0.8 (13±5)	67.6±1.5 (69±7)	17.7±1.3 (18±7)	2.1±0.7							34.08
86				4.8±1.0 (4±1)	60.4±2.0 (62±10)	29.3±1.5 (31±10)	5.5±1.0 (3±1)							34.36
87				2.0±1.0 (1±)	27.8±1.2 (39±7)	51.4±1.8 (44±7)	17.2±1.0 (15±1)	1.6±1.0						34.89
88				1.0±0.5	10.1±1.0 (11±1)	39.9±2.0 (51±3)	46.6±2.0 (37±3)	2.4±0.8 (1±)						35.39
89					2.2±0.8 (2.3±1)	24.8±1.4 (26±4)	67.5±2.0 (67±4)	4.8±0.9 (4.7±1.6)	0.7±0.6					35.77
90						10.0±0.7 (11±2.5)	75.9±1.0 (76±3)	14.1±0.7 (13±2)						36.04
91						4.0±0.5 (4.0±1.6)	53.9±1.0 (55±1.5)	37.6±1.0 (38±3)	4.5±0.5 (3±3)					36.43
92						1.8±0.8	31.5±1.4 (31±1)	50.4±1.8 (55±3)	15.2±1.4 (14±3)	0.9±0.6	0.2±0.2			36.82
93							10.7±1.2 (8±1)	48.8±1.7 (49±3)	37.9±1.5 (41±3)	2.6±0.7 (1.6±0.2)				37.32
94							3.1±0.8 (2.7±0.5)	24.8±1.2 (25±1.5)	65.2±1.8 (66±2.5)	6.3±0.8 (6±2)	0.6±0.5			37.77
95							0.9±0.5	13.7±1.5 (10±0.5)	68.4±2.0 (77±6)	15.4±1.5 (13±6)	1.6±0.8			38.03
96								4.9±1.0 (2.1±0.1)	58.4±2.5	32.2±2.5	3.5±0.8	1.0±0.8		38.37
97								3.5±1.0 (0.6±0.1)	30.7±2.0	54.1±2.0	10.6±1.5	1.1±0.6		38.75
98								0.9±0.6	15.0±2.2	37.7±3.0	43.4±3.0	3.0±1.5		39.33
99									6.2±1.2	34.3±2.5	53.6±2.5	4.6±1.2	1.3±0.8	39.61
100									0.9±0.6	8.8±1.2	82.9±3.0	6.5±0.9	0.9±0.6	39.98

A. Moments of the nuclear charge distribution

For each mass number the yields obtained for the different nuclear charges are listed in Table I. These yields were averaged for each isobar over the kinetic energies and ionic charges with the isobaric yields for the different kinetic energies and ionic charges being used as weighting factors as in Refs. 8 and 9. In order that the contributing kinetic energies U and ionic charges q can be traced back we have listed in Table II the U and q values of all measurements that were used for the averaging process.

In cases where a strong dependence of the nuclear charge distribution was observed for different kinetic energies and ionic charges, up to 21 measurements were performed for one isobaric chain. In that extremal case about one-half of the total yield of one mass contributed to the final result.

For nuclear physics it is of no direct interest to measure the influence of the ionic charge on the yield of particles of one nuclear charge within one isobaric chain. It is necessary, however, to record this dependence since, for a given mass and kinetic energy, the ratio of the yields of two adjacent nuclear charges can change by a factor of 2 if the ionic charge is one unit away from its average value.[9] This can be of special importance if the average nuclear charge has a noninteger value or if at that ionic charge no pure beam of fission products can be obtained due to the separation principle of the recoil separator.[5]

The yield for the different nuclear charges $Y(A,Z)$ as well as the average nuclear charges $Z_a(A)$ is given in Table I for the isobars $A = 79$ to $A = 100$. The values for $A = 90$ to $A = 100$ are here slightly improved over the data reported in Ref. 8 by using additional measurements. For comparison the radiochemically obtained nuclear charge yields are given in brackets according to a recent compilation.[16,17] The general agreement is good.

There is also partial agreement between the data presented here and those for fission products of selected kinetic energy and ionic charge as given in Ref. 13. As is expressed there, an agreement cannot be expected a priori. The better agreement between the data presented here and those given in Ref. 17 can be expected from the averaging process. Such a comparison shows for instance that the average nuclear charges given in Ref. 13 have the tendency to be higher than those of Ref. 17 or those presented here.

From the observed nuclear charge distributions a correction factor for Wahl's normal distribution could be derived similarly as in Ref. 17. Follow-

ing this idea the yield Y of the nuclear charge Z in the mass chain A should be described by

$$Y(A,Z) = Y_{\text{Wahl}}(A,Z)(1 + 0.19\delta_p + 0.04\delta_n), \qquad (1)$$

where $Y_{\text{Wahl}}(A,Z)$ is Wahl's normal distribution[1] and δ_p and δ_n are equal to $+1$ or -1 depending on whether A has an even or an odd proton or neutron number, respectively. As can be seen from Eq. (1), the enhancement due to an even neutron number thus is about five times smaller than the enhancement due to an even proton number. The result of both correction factors should be more exact than the correction factor $(1 + 0.25\delta_p)$, given in Ref. 17, which took into account only the proton pairing.

While the detailed results for the nuclear charge distribution are listed in Table I all interesting features of it are displayed in Fig. 2 as a function of the post-neutron emission mass. All lines shown are drawn to guide the eye.

1. Average nuclear charge

The average nuclear charge $Z_a(A)$ for different masses is displayed in Fig. 2(a). Even nuclear charges are indicated by thin horizontal lines. The change of the average nuclear charge with mass is smallest if it is close to an even charge value and largest in the middle between two even values. As an example, two slopes are indicated by dashed lines. The average slope in the mass region of Fig. 2(a) at even proton numbers is

$$\Delta Z_a / \Delta A = 0.33 \pm 0.02$$

and

$$\Delta Z_a / \Delta A = 0.53 \pm 0.03$$

at odd proton numbers. This indicates that the average nuclear charge Z_a stays close to an even value as long as possible. When it leaves this value it changes rapidly to the next even proton number.

In the best established region of radiochemical results ($A = 89$ to $A = 95$) the average nuclear charges Z_a were averaged for the radiochemical data as well as for our data of Table I. The result was that the average of our Z_a was about 0.006 charge units higher than the average of the radiochemically obtained Z_a of Ref. 16. This is a remarkable agreement between radiochemical data and the here reported results. The values of Z_a for $A < 89$ were not taken into account since there were several changes from Ref. 16 to Ref. 17.

2. Width of the nuclear charge distributions

The rms widths σ of the nuclear charge distributions are plotted in Fig. 2(b). As reported al-

G. SIEGERT *et al.*

TABLE II. The ionic charges q and energies U of all measurements which contributed to the averaged independent yields for each mass are listed as q/U (a sizable portion of points has been measured several times so that about twice as many measurements were performed as listed).

q/U

A																
79	19/81.6	19/87.6	19/87.6													
80	19/81.6	19/87.6	19/87.6	21/84.6												
81	18/85.7	18/92.3	19/81.6	19/87.6	21/84.6											
82	19/84.6	19/89.6	19/94.6	20/90.7	22/90.7	23/90.6										
83	19/90.7	20/79.6	20/84.6	20/89.6	20/94.6	22/90.7	23/90.6									
84	18/75.8	19/90.7	20/79.7	20/84.5	20/89.4	20/90.7	20/94.5	22/90.7	23/90.6							
85	19/80.0	19/90.7	20/74.7	20/79.7	20/84.3	20/84.6	20/89.6	20/90.7	20/94.6	20/99.6	22/90.7	23/90.6				
86	18/89.5	18/89.6	19/80.0	19/89.6	20/73.3	20/74.7	20/80.6	20/84.6	20/87.9	20/89.8	21/89.6	22/89.8	23/89.7	23/90.6		
87	19/80.0	19/90.7	20/79.7	20/84.6	20/89.6	20/90.7	20/94.6	20/99.6	23/90.6							
88	19/90.7	20/79.7	20/84.3	20/87.9	20/89.6	20/90.7	20/94.6	20/95.3	20/99.6	20/102.6	21/88.5	21/90.4	21/92.9	21/99.9	23/90.6	23/95.1
89	19/75.7	19/80.0	19/86.1	20/69.7	20/76.2	20/79.7	20/84.3	20/84.6	20/88.5	20/89.6	21/85.4	21/90.4	21/92.3	21/99.9	23/95.1	
90	18/75.8	19/80.0	20/73.3	20/80.6	20/83.3	20/84.3	20/87.9	20/88.5	20/95.1	20/95.3	21/87.6	21/93.6	21/95.1	21/99.6		
91	19/80.0	19/90.5	20/79.7	20/84.3	20/88.5	20/90.6	21/77.0	21/87.6	21/88.5	21/90.4	21/92.9	21/95.1	22/80.6	22/92.7		
92	19/80.0	20/73.3	20/80.6	20/84.3	20/87.9	20/95.3	20/102.6	21/88.5	22/92.7	22/97.3						
93	17/81.1	20/84.3	21/92.7	22/92.9	22/97.3	23/84.3										
94	17/81.1	19/80.0	20/73.3	20/80.6	20/84.3	20/87.9	20/95.3	20/102.6	21/88.5	21/92.9	21/100.2	22/92.7	22/97.3	23/84.3		
96	20/84.3	21/88.5	21/92.9	22/92.7												
97	21/88.5	21/92.9	22/92.7	22/97.3	23/96.9											
98	21/88.5	21/92.9	22/97.3	22/97.3												
99	20/84.3	22/80.6	22/92.7	22/97.3	22/99.7	23/96.9	23/101.1									
100	19/90.6	20/84.3	21/88.5	21/92.9	22/93.7	22/97.1	22/99.7	23/91.6	23/97.3	23/103.0	23/104.3					

FIG. 2. Different aspects of the nuclear charge distri-
bution of fission products are shown graphically as func-
tions of the particle mass. (a) The average nuclear
charge is plotted. Note the steeper slopes at odd Z_a
and the not so steep ones at even Z_a. (b) The rms
width σ of the nuclear charge distributions is shown.
Note the minimal σ (most narrow distribution) at $A = 80$,
90,100 which have even-even center nuclei in the nu-
clear charge distributions and the maximal σ (most
wide distributions) at $A = 82,88,92,98$ which have odd-
odd center nuclei in the nuclear charge distributions.
(c) The skewness of the nuclear charge distributions is
shown. For Z_a being an integer value the skewness
always vanishes indicating that in these cases the nu-
clear charge distribution is symmetric. (d) The excess
of the nuclear charge distributions is shown. For $A = 80$,
85,90,95,100 the excess is largest. Together with the
vanishing skewness at these masses this indicates a
maximal deviation of the nuclear charge distribution
from a Gaussian for mass chains characterized by an
even proton center nucleus.

ready in Ref. 8 the nuclear charge distributions
are especially narrow when their central nuclear
charge falls on an even proton number, resulting
in especially small values for σ.

This regular variation of σ with the mass A is

found to continue[11] in the mass range $79 \leq A \leq 89$
beyond the already reported region $90 \leq A \leq 100$.
The σ values for $A = 84$ and $A = 85$, however, are
somewhat off the expected curve. This deviation
can be attributed[9] to the influence of the $N = 50$
shell. For $A = 84$ the yield of the central nucleus
$^{84}_{34}Se_{50}$ is favored not only because of its even pro-
ton and even neutron number, but in addition be-
cause of its closed neutron shell $N = 50$. Thus an
exceptionally narrow nuclear charge distribution
results for $A = 84$ and thus an exceptionally small
σ.

This effect is indicated by the downward arrow
in Fig. 2(b). For $A = 85$ the even proton number
favors $^{85}_{34}Se_{51}$ whereas the $N = 50$ shell favors the
neighboring nucleus $^{85}_{35}Br_{50}$, thus causing a larger
width of the nuclear charge distribution indicated
by the upward arrow in Fig. 2(b). The broken
curve in that region indicates the expected σ values
without the influence of the $N = 50$ shell.

Though the main variation of the rms width in
the nuclear charge distributions is due to the pro-
ton pairing, there is some influence from the neu-
tron pairing too. For even proton numbers ac-
companied by even neutron numbers (A being 80,
90,100) the central nuclide is favored causing the
distributions to be especially narrow and the cor-
responding σ values to be especially low. When
only the proton pairing favors the central nuclide
and the neutron pairing favors both neighbors
$[A = 85$ (the $N = 50$ shell effect being subtracted)
and $A = 95]$ one finds larger σ values. For odd
proton numbers of the central nuclide rather wide
nuclear charge distributions must be expected. If
such a central nuclide has additionally an odd neu-
tron number, the nuclear charge distribution is
widest ($A = 82,88,92,98$). Thus, on the general
periodicity of 5 mass units, a 6-4-6 periodicity
is superimposed. This periodicity is well estab-
lished not only on the average but also in going
from one mass to the next one. To see this we
may go from any one of the masses (A being 82,
88,92,98) each characterized by an odd-odd center
nuclide to the neighbor which is characterized by
a center nuclide for which the proton number is
still odd but the neutron number is even, i.e.,
from $A = 82$ to $A = 83$, from $A = 88$ to $A = 87$, from
$A = 92$ to $A = 93$, and from $A = 98$ to $A = 97$. In three
cases we find a reduced σ and thus a narrower
nuclear charge distribution as postulated by the
6-4-6 periodicity due to the neutron odd-even ef-
fect.

In general the width 2σ of the nuclear charge
distribution seems to increase slightly with mass
A or nuclear charge Z [see the slightly inclined
lines I, II, III in Fig. 2(b)] so that the relative
widths σ/A or σ/Z are nearly constant. This can

be explained by the fact that for increasing mass or nuclear charge the relative change in all properties decreases in going from one nuclide to any of its neighbors. For the same available energy among heavier masses the energetically less favored nuclides get a bigger chance to be formed compared to lighter nuclei. Apart from this general trend all the details of Fig. 2(b) are explainable by proton and neutron pairing. The contribution from neutron pairing cannot be separated at that stage into that due to the fission process and that due to neutron evaporation.

Another interesting feature of Fig. 2(b) is the increase of σ around $A = 90$ above the general trend indicated by the slightly inclined thin lines marked with roman numerals I to III. This local effect is hard to explain by a corresponding change in the preference for one nuclear charge. One idea might be that in this region more energy is available for pair breaking than in other areas so that around $A = 90$ larger widths of the nuclear charge distributions must be expected. Another, in our view more probable, explanation would be that the neutron odd-even effect observed after the neutron evaporation depends on the average number of evaporated neutrons. As long as zero or two neutrons are emitted one naturally expects no effect, but as soon as only one neutron is emitted, one observes with higher yield a nucleus which originally had an even neutron number but which now has an odd one. Around the mass 90 the most probable number of evaporated neutrons[18] is around 1; thus a slightly wider nuclear charge distribution could be expected in this region.

3. Skewness of the nuclear charge distributions

The skewness $S = \mu_3/\sigma^3$ (with μ_3 being the third moment) of the nuclear charge distributions is plotted in Fig. 2(c). The skewness is 0 if the value of the average nuclear charge Z_a has integer values (even or odd) corresponding to average mass values of about 80, 82.5, 85, 87.5, 90, 92.5, 95, 97.5, and 100. For mass values in between, the skewness is largest with a sign that favors the next even nuclear charge. It can be concluded therefore that the skewness of the nuclear charge distribution is a result of the proton pairing. The skewness oscillates around zero in this mass interval. In other words, the nuclear charge distribution on the average is symmetric. The tendency for the average nuclear charge to jump to the next even proton number is as strong as that to stick to the former one.

In the skewness of the nuclear charge distribution clearly the effect of the $N = 50$ shell can also be seen. For $A = 83$ we would expect already a

negative skewness, expressing the fact that already the next higher nuclear charge is favored. We find, however, a still positive skewness since the $^{83}_{33}\text{As}_{50}$ nucleus favored by $N = 50$ lies on the left side of the nuclear charge distribution. For $A = 84$ we would expect a reasonable negative skewness; we find, however, a rather large negative one. Here the favored nucleus with $N = 50$, i.e., $^{84}_{34}\text{Br}_{50}$, lies at the side of the higher nuclear charge. The rapid change of the skewness between $A = 83$ and $A = 84$ thus can be attributed to the influence of the $N = 50$ neutron shell [see also the arrows in Fig. 2(c)].

4. Excess of the nuclear charge distribution

The excess $E = (\mu_4/\sigma^4) - 3$ (with μ_4 being the fourth moment) of the nuclear charge distributions is shown in Fig. 2(d). For A being 80, 85, 90, 95, and 100 the excess is largest indicating that the nuclear charge distribution is sharper peaked than a Gaussian if the central nucleus has an even proton number. Between these values, when the central nucleus is not favored, the excess comes to 0. For A being 83, 87, 93, and 97 the skewness and the excess are smallest; therefore, the nuclear charge distribution of these isobars is closest to a Gaussian. Contrary to the average skewness the average excess is not zero over the investigated mass interval, indicating that the nuclear charge distributions on the average are sharper peaked than a Gaussian.

The excess at around $A = 90$ is especially low. This is in agreement with the conclusion drawn from the rms width of the nuclear charge distribution of Fig. 2(b). As the pairing energy should stay constant to first order one may try to explain this observation as in Sec. III A 2 either by assuming that the available excitation energy is higher for these masses or by assuming that for masses around $A = 90$ about one neutron is evaporated thus washing out the neutron odd-even effect to some extent.

The influence of the proton pairing can be seen up to the fourth moment. When the average nuclear charge is even (indicated by the vertical lines in Figs. 2) the rms width is smallest and the excess is largest. The skewness is 0 if the average nuclear charge Z_a is even (preferred), or if it is exactly between two preferred even values, i.e., Z_a is odd. The sign of the skewness shows that the next even proton number is strongly preferred.

B. Distributions derived from the nuclear charge measurements

1. Wahl's diagram

In Fig. 3 the conventional Wahl diagram is shown. The average nuclear charge is plotted
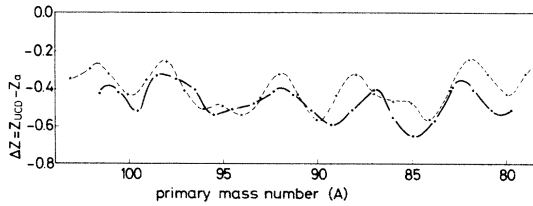
FIG. 3. Wahl's diagram is shown for all observed Z_a. The dotted curves represent the corresponding ΔZ as calculated in Ref. 19. The agreement is satisfying within the assumptions of the theory. More clearly than from the theoretical curve the small ΔZ values can be seen to occur for the even proton center nuclei with $A = 80, 85, 90, 95, 100$.

against the pre-neutron emission mass. Included also in this figure are theoretical values obtained in Ref. 19. In order that this diagram can be directly compared with other diagrams of this type we have used Wahl's prescription together with the values of the average number of evaporating neutrons as a function of mass. In the preceding section we have seen how deeply the proton and neutron pairing influences the moments of the nuclear charge distribution. Therefore it can also be expected that the average nuclear charge shows a corresponding pattern. Attention to this point was first drawn in Ref. 10, where the average nuclear charge was given for fission products of selected kinetic energy and ionic charge. The data of Ref. 8 as well as the data here, which both reveal the effect a little more clearly, represent fission particles of all ionic charges and kinetic energies. This plot therefore should give the same pattern as for data obtained by radiochemical methods. For comparison the corresponding values calculated in Ref. 19 are shown, which exhibit similar structure.

2. Element and isotone yields

The yields for different elements summed over all contributing mass chains given in Fig. 4 were shown already.[9,10,13,16] The chain yields in our case were taken from Ref. 20. In Ref. 9 as well as for the curve of Fig. 4 we have used for the masses 101 to 106 our results taken at the average kinetic energies and close to average ionic charge. The averaged proton odd-even effect of Fig. 4 is

$$\frac{2\Sigma Y(Z = \text{even})}{\Sigma Y(Z = \text{even}) + \Sigma Y(Z = \text{odd})} = 1.22 \pm 0.01 \qquad (2)$$

which is in perfect agreement with Refs. 13 and 16.

The yields for different isotones summed over all contributing mass chains given in Fig. 5 were shown in Ref. 9 and later in Ref. 13. The chain yields in our case again were taken from Ref. 20.
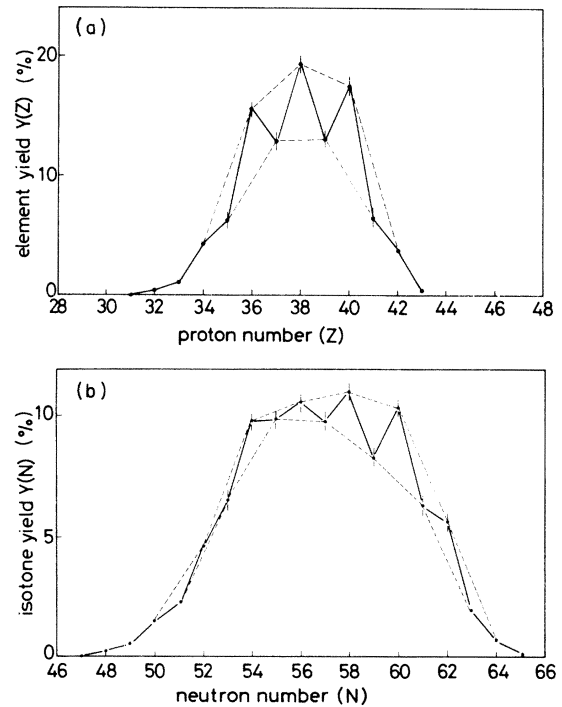
FIG. 4. The element (a) and the isotone (b) yields are shown as a function of proton and neutron numbers, respectively. Note the about constant odd-even effect for the element yield and the (with N) increasing odd-even effect for the isotone yield.

Also here we have used, for the masses 101 to 106, our results taken at the average kinetic energies and close to average ionic charges.

The average neutron odd-even effect of Fig. 5 is

$$\frac{2\Sigma Y(N = \text{even})}{\Sigma Y(N = \text{even}) + \Sigma Y(N = \text{odd})} = 1.09 \pm 0.01. \qquad (3)$$

The corresponding value in Ref. 13 was 1.08 ± 0.01, whereas in Ref. 16 this value was only found to be smaller than 1.03 for the range of $N = 52$ to $N = 57$.

The odd-even effects of Figs. 4 and 5 prevail if, for the different isobaric chains, the same isobaric yields were always assumed. Thus it seems clear that the observed odd-even effects are really due to the number of protons and neutrons but not due to possibly preferred combinations of them which should favor certain mass numbers over others.

3. Variation of the proton and neutron odd-even effect with mass

The odd-even effect of the element distribution and of the isotone distribution can be seen qualitatively in Fig. 4 (dashed curves). To get a more quantitative picture the odd-even effect has been
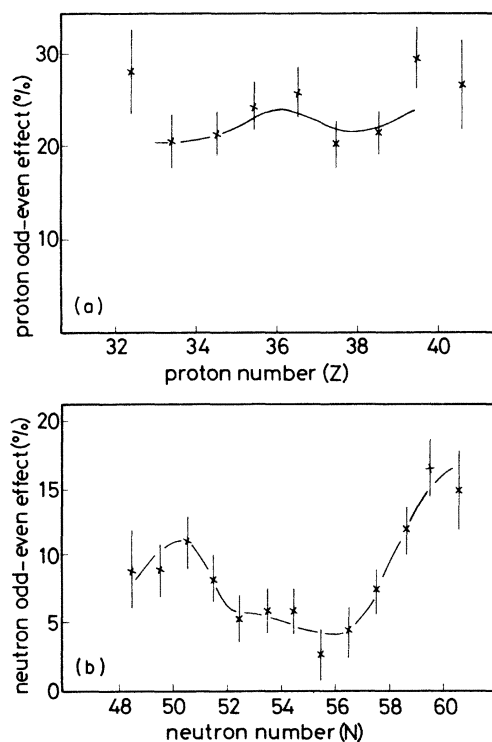
FIG. 5. The proton and neutron odd-even effects.
Note that no clear minimum is seen for the proton odd-
even effect; however, a clear minimum shows up in
the neutron odd-even effect.

calculated from Fig. 4 according to Ref. 21. The
results are shown in Fig. 5. They must be com-
pared to corresponding results of Ref. 13 which
were obtained from fission products of selected
kinetic energy and ionic charge. It can be ex-
pected that these additional conditions and the
approximation used there lead to different results.

From our measurements it must be concluded
that the proton odd-even effect is almost indepen-
dent of the proton number. It certainly does not
show such an expressed minimum as in Ref. 13
around the most probable mass split. This min-
imum was attributed there to a higher excitation
energy which should be available for nuclei close
to the most probable mass split. In addition to the
small not very significant minimum around the
most probable mass split ($Z \simeq 38$) we find an also
quite low value of the proton odd-even effect for
$Z \simeq 34$ where the mass yield has dropped to one-
fifth. Therefore, other influences are present
which are at least as strong as that one due to

the most probable mass split.

The neutron odd-even effect in our measure-
ments shows a peak around $N = 50.3$. A correspond-
ing maximum is found in Ref. 13 at $N = 51.0$. At
least part of the peak reported here is due to the
$N = 50$ shell. The calculation of the odd-even effect
asks for four consecutive isotone yields and smears
out the effect of a closed neutron shell over four
neutron numbers. The effect of such a closed
neutron shell thus can be seen much more pre-
cisely from the moments of the nuclear charge
distribution as is demonstrated above.

The neutron odd-even effect is much smaller
than the proton odd-even effect, especially be-
tween $N = 52$ and $N = 56$. This can be attributed to
the neutron evaporation which washes out the pri-
mary hitherto unknown neutron odd-even effect.
How much this effect is washed out may very well
depend on the average number of emitted neutrons
as outlined in Sec. III A 2. It can be expected that
this effect contributes to the dependence of the
neutron odd-even effect and gives some underlying
trend.

IV. SUMMARY

The measurement of the nuclear charge distri-
butions averaged over kinetic energy and ionic
charge has revealed how strong the influence of
the odd-even effect in fission is and how far it
can be followed. The rms widths of the nuclear
charge distributions are mainly governed by the
proton pairing effect. Smaller details are explained
by the neutron pairing and by the influence of the
$N = 50$ shell. The skewness of the nuclear charge
distributions is due to proton pairing and due to
the $N = 50$ shell. The excess of the nuclear charge
distributions is caused by proton pairing and shows
that the average nuclear charge distribution is
sharper peaked than a Gaussian. The already ac-
cepted[16] proton odd-even effect in the element dis-
tribution is confirmed with higher precision. The
neutron odd-even effect already shown in Ref. 9
is established without approximations and addition-
al conditions for the whole fission process.

*Institut Laue-Langevin, 38 Grenoble, France.

†In partial fulfillment of the requirements for the degree of Dr. rerum naturalium.

[1] A. C. Wahl, A. E. Norris, R. A. Rouse, and J. C. Williams, in *Proceedings of the Second International Atomic Energy Agency Symposium on Physics and Chemistry of Fission, Vienna, 1969* (IAEA, Vienna, 1969), p. 813.

[2] H. Gunther, G. Siegert, R. L. Ferguson, and H. Ewald, Nucl. Phys. A196, 401 (1972).

[3] E. Konecny, H. Gunther, H. Rösler, G. Siegert, and H. Ewald, Z. Phys. 231, 59 (1970).

[4] K. Sistemich, P. Armbruster, J. Eidens, and E. Röckl, Nucl. Phys. A139, 289 (1969).

[5] E. Moll, H. Schrader, G. Siegert, J. P. Bocquet, G. Bailleul, J. P. Gautheron, J. Greif, G. I. Crawford, C. Chauvin, H. Ewald, H. Wollnik, P. Armbruster, G. Fiebig, H. Lawin, and K. Sistemich, Nucl. Instrum. Methods 123, 615 (1975).

[6] G. Siegert, H. Wollnik, J. Greif, G. Fiedler, M. Asghar, G. Bailleul, J. P. Bocquet, J. P. Gautheron, H. Schrader, H. Ewald, and P. Armbruster, Phys. Lett. B53, 45 (1974).

[7] H. C. Clerc, K. H. Schmidt, H. Wohlfarth, W. Lang, H. Schrader, K. E. Pferdekämper, R. Jungmann, M. Asghar, J. P. Bocquet, and G. Siegert, Nucl. Instrum. Methods 124, 607 (1975).

[8] G. Siegert, J. Greif, H. Wollnik, G. Fiedler, R. Decker, M. Asghar, G. Bailleul, J. P. Bocquet, J. P. Gautheron, P. Armbruster, and H. Ewald, Phys. Rev. Lett. 34, 1034 (1975).

[9] G. Siegert, H. Wollnik, J. Greif, R. Decker, G. Fiedler, B. Pfeiffer, M. Asghar, J. P. Bocquet, C. Chauvin, G. Bailleul, and H. Schrader, in Proceedings of the Spring Meeting of the German Physical Society, Den Haag, 1975 (unpublished).

[10] H. G. Clerc, K. H. Schmidt, H. Wohlfarth, H. Schrader, K. E. Pferdekämper, R. Jungmann, M. Asghar, J. P. Bocquet, and G. Siegert, in Proceedings of the Spring

Meeting of the German Physical Society, Den Haag, 1975 (unpublished).

[11] H. Ewald and H. Wollnik, in Proceedings of the Fifth International Conference on Atomic Masses and Fundamental Constants, Paris, 1975 (AMCO-5), edited by A. H. Wapstra (Plenum, New York, to be published).

[12] H. G. Clerc, K. H. Schmidt, H. Wohlfarth, W. Lang, H. Schrader, E. K. Pferdekämper, R. Jungmann, M. Asghar, J. P. Bocquet, and G. Siegert, Nucl. Phys. A247, 74 (1975).

[13] H. G. Clerc, W. Lang, H. Wohlfarth, K. H. Schmidt, H. Schrader, K. E. Pferdekämper, and R. Jungmann, Z. Phys. A274, 203 (1975).

[14] G. Siegert, J. Greif, H. Wollnik, R. Decker, G. Fiedler, W. Kaiser, and B. Pfeiffer, Institut Laue-Langevin Report No. 75 S 219 S, 1975 (unpublished).

[15] S. Neumann and H. Ewald, Z. Phys. 169, 224 (1962); H. Wollnik, Ph.D. thesis, Munich, 1964 (unpublished); H. Wollnik, G. Fiebig, and H. Lawin, in Discussion Meeting on Neutron Physics, Kernforschungsanlage Jülich, Jülich, 1967 (unpublished), p. 220.

[16] S. Amiel and H. Feldstein, in *Proceedings of the Third International Atomic Energy Agency Symposium on Physics and Chemistry of Fission, Rochester, 1973* (IAEA, Vienna, 1974), Vol. II, p. 65.

[17] S. Amiel and H. Feldstein, Phys. Rev. C 11, 845 (1975).

[18] H. Niefenecker, C. Signarbieux, R. Babinet, and J. Poitou, in *Proceedings of the Third International Atomic Energy Agency Symposium on Physics and Chemistry of Fission, Rochester, 1973* (see Ref. 16), Vol. II, p. 117.

[19] B. D. Wilkens and E. P. Steinberg, Phys. Lett. 42B, 141 (1972).

[20] W. Seelmann-Eggebert, G. Pfennig, and H. Münzel, *Nuklidkarte* (Gersbach, München, 1974), 4th ed.

[21] B. L. Tracy, J. Chaumont, R. Klapisch, J. M. Nitschke, A. M. Poskanzer, E. Roeckel, and C. Thibault, Phys. Rev. C 5, 222 (1972).